FUNCTIONAL ROLE OF THE CONNECTIVE TISSUE AND THE GAP JUNCTION DISTRIBUTION IN THE SINUS NODE

Per Östborn

Department of Mathematical Physics, Lund University, S – 222 00 Lund, Sweden

Abstract

Sinus node (SN) cells are intermingled with a great amount of connective tissue, and are coupled with few and small gap junctions. Though, SN cells close to impulse exit sites from the node seem to be more strongly coupled than are interior cells. The functional significance of these properties is unclear. We put forward the hypothesis that these qualities help the SN resist the hyperpolarising drain current to the atrium. To test the hypothesis, we study a simple model consisiting of a group of SN cells coupled to a row of atrial cells. Simulations show that in this model, the SN cells resist the drain better if they are more weakly coupled, in the sense that they then drive the atrial cells at a higher frequency. If some pairs of SN cells in the group are electrically disconnected, simulating the presence of connective tissue strands, the cell group drives the atrium at a given ideal frequency at a higher coupling conductance gSS between the cells that are still connected. This leads to an increase of the safety factor $gSS/gSS_{\min}$ towards the minimum coupling conductance $gSS_{\min}$, below which the atrium cannot be driven. Higher coupling between the most peripheral SN cells also increases this safety factor. A sudden coupling increase is better than a gradual one in this respect. In conclusion, the simulations support the hypothesis that the SN qualities mentioned above have developed to maintain a proper and safe pacemaker function in the presence of the hyperpolarising current to the atrium.

1. Introduction

In this paper, we put forward the hypothesis that some sinus node (SN) qualities have evolved to protect the SN from the hyperpolarising drain current to the atrium. We use qualitative simulation and argumentation to support the hypothesis.

1.1. Experimental background to the SN qualities of interest

Rabbit SN cells are coupled with fewer and smaller gap junctions than other myocardial cells (Bleeker et al., 1980; Masson-Pévet et al., 1979). Immunohistochemical labelling of the gap junction protein Cx43 shows a sharp border between the SN, which is mostly Cx43-negative, and the Cx43-positive atrium (Coppen et al., 1999; Kwong et al., 1998; Oosthoek et al., 1993; ten Velde et al., 1995; Verheijck et al., 2001).

SN myocytes are placed in a dense, irregularly arranged network of connective tissue (De Mazière et al., 1992; James, 1977; Bharati and Lev, 1988). De Mazière et al. (1992) investigated the possible role of this tissue for impulse propagation, but found no gap junctions connecting SN cells to fibroblasts. Calculations showed that the fibroblasts therefore cannot participate in impulse transmission. The connective tissue thus seems to be electrically insulating.

As noted above, most SN cells are Cx43-negative and there is a sharp transition to Cx43-positive atrial cells. However, Kwong et al. (1998) found Cx43-positive bundles of canine SN cells, which seemed to abut atrial cells. In the rabbit, Coppen et al. (1999) found a restricted zone close to the crista terminalis where SN cells expressed Cx43. Verheule et al. (2001) also found Cx43-positive rabbit SN cells close to the SN periphery. This suggests that SN cells close to impulse exit sites are more well coupled. An earlier study (Bleeker et al., 1980) indicated a gradual increase in the number and size of gap junctions in the rabbit SN periphery towards the crista terminalis.

In the simulations, a sharp sino-atrial (SA) border separating distinct cell types is assumed. This is supported by the distinct staining patterns of Cx43. Verheijck et al. (1998) found no intermediate rabbit cell types between the purely nodal and purely atrial ones.

1.2. The drain current to the atrium

The hyperpolarising drain current has been demonstrated indirectly in experiments (Bouman et al., 1994; Kirchhof et al., 1987). It arises because the maximum diastolic potential (MDP) of SN cells is less negative than the atrial cell resting potential. The drain makes the

firing frequency lower since the diastolic depolarisation becomes slower. For high enough drain current, SN cells become quiescent (Watanabe et al., 1995).

By disconnecting rabbit SN from the atrium, Kirchhof et al. (1987) showed that the atrium caused the SN frequency to decrease 18% in the mean, suggesting that the drain plays a significant role for the function of the SN. One could also try to estimate the importance of the drain by means of simulations. But Joyner and Van Capelle (1986) have pointed out that simulation results depend heavily on the excitability of the atrial cells, since this determines how large the sino-atrial (SA) coupling has to be, and on the ability of SN cells to withstand the drain. This ability is related to the strength of the hyperpolarisation-activated current i_h. Also, the impact of the drain depends on the difference between the SN cell MDP and the atrial cell resting potential. Joyner and Van Capelle (1986) had to use a model SN of considerable size to be able to drive the atrium, whereas Boyett et al. (1995) found that a single model SN cell could drive a model atrial cell at reasonable frequency no matter how large the SA coupling was. In a study by Joyner et al. (1998), where a model SN cell was coupled to a real atrial cell, it was found that the atrial cell could be driven at a reasonable frequency by the SN cell. However, one should keep in mind that in the latter two studies, only a single atrial cell was used. This makes the MDP of this cell less negative than would be the case if it was coupled to additional atrial cells, to which the depolarising drain current from the SN cell could be dissipated. Therefore the drain becomes more severe in multicellular atrial tissue.

1.3. Previous studies of SN qualities in relation to the drain current

Several studies have focused on the functional pressure that the drain current exerts on the SN. In the simulation study by Joyner and van Capelle (1986), it was shown that when the SN was partially insulated as a protection against the drain, a gradual *decrease* in coupling between *atrial cells* going towards the SA junction helped the SN trigger the atrium. To my knowledge, such an arrangement has not yet been found experimentally. (For comparison, in this study, we investigate the possible advantage of *increasing* the coupling between *SN cells* close to the SA junction.)

In the search for qualities of the SA border that could help the SN resist the drain, it has been found that the atrium apparently forms narrowing strands that penetrate into the SN, and that the SN seems to be significantly coupled to the atrium only at the tips of these strands (Oosthoek et al., 1993; ten Velde et al., 1995). The narrowing strands means that the SN cells

at the strand tips only have to trigger an essentially one-dimensional string of atrial cells, as would be the case if gap junctions were dense all over the SA border. Thus a great deal of the SN can be electrically disconnected from the atrium without having to increase the conductance through the remaining impulse outlets. The total drain experienced by the SN diminishes.

Peripheral SN cells are more forceful, with increased densities of several ion channels and higher natural frequencies compared to central SN cells (Boyett et al., 1999; Boyett et al., 2000; Kodama and Boyett, 1985; Opthof et al., 1987; Zhang et al., 2000). These should therefore be better suited to resist a given amount of drain than are interior cells. Specifically, Zhang et al. (1998) found in a simulation study that if the sodium channels were removed from the SN periphery, the atrium could no longer be driven. This could explain the increased density of sodium channels in the SN periphery that is found experimentally (Boyett et al., 2000).

2. Methods

In the modelling, we do not try to relate gap junction conductances and element capacitances to real cellular values. This is because model studies that do so, nevertheless have difficulties to estimate the impact of the drain current, as discussed above. For this reason, the word "element" will be used in the following instead of "cell". In other words, we do not try to determine how many cells are contained in each element.

2.1. The single-element model

The Irisawa-Noma model (Irisawa and Noma, 1982) was used to simulate SN elements. There are several more modern and exact models available, but since our aim is qualitative, we choose to use the simplest model based on experiments on SN cells.

Since a time-consuming integration method is needed (see below), the Irisawa-Noma model is simplified to speed up integration. The Na-channel is removed, and the Ca-channel activation variable d is set to its steady state value d_∞. These operations are justified since the Na-current is always very small (Irisawa and Noma, 1982), and d adjusts very quickly to d_∞ (Guevara et al., 1987). Fig. 1 shows potential traces of the complete and simplified Irisawa-Noma models.

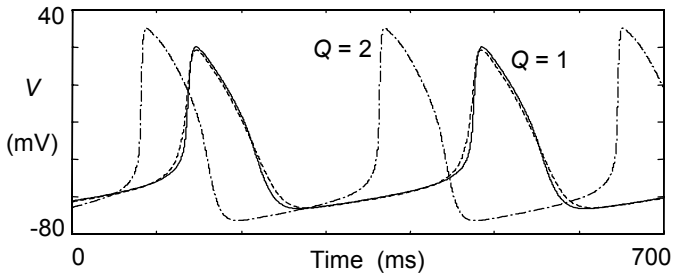

Fig. 1. Potential traces of different versions of the Irisawa-Noma model (Irisawa and Noma, 1982). The dashed curve corresponds to the complete model, the solid curve to the simplified model, and the dash-dotted curve to the simplified model with the densities of Ca- and K-channels doubled ($Q = 2$). The doubling of these densities produces higher frequency (282 ms compared to 338 ms), more negative maximum diastolic depolarisation, higher overshoot, and higher upstroke velocity. This is in accordance with the experimental record (Boyett et al., 1999; Boyett et al., 2000; Kodama and Boyett, 1985; Opthof et al., 1987).

We want to model the behaviour of SN cells close to the SA junction. It has been reported that in the rabbit, these cells have higher natural frequency than those in the SN centre cells (Boyett et al., 1999; Boyett et al., 2000; Kodama and Boyett, 1985; Opthof et al., 1987). We found that in the simplified model, the corresponding change in the potential waveform is well reproduced if the membrane densities of Ca- and K-channels both increase by a factor $Q = 2$. Therefore this operation is performed for all SN elements in most simulations below. Fig. 1 shows potential traces of the simplified model before and after the operation. Detailed models of peripheral and central SN cells have been developed by Zhang et al. (2000), based on the existing experimental evidence regarding the regional differences in the densities of membrane currents. This knowledge is not complete, however. In these models, the densities of almost all channels are increased in the periphery, including the hyperpolarisation activated channel. In the present model, better fit with the experimental record is obtained if this channel is left unchanged.

Non-automatic (atrial) elements are simulated with the membrane model introduced by Wohlfart and Arlock (1993), with the parameter values used by Östborn et al. (2001a).

2.2. The multi-element model

When we construct the multi-element model, our philosophy is to use the *simplest possible model* from which (hints of) answers to our questions can be gained. In all simulations, the system in Fig. 2 is used. A cube of eight SN elements is coupled to a row of six atrial elements. The SN elements are coupled according to one of the graphs in Fig. 3. The coupling conductance between SN cells is denoted by *gSS*. The SN is coupled to the atrium with

conductance *gSA*, and the atrial elements are coupled with a common conductance *gAA*. If only one atrial element is used, it is hard to tell whether the excitation will survive or not, while the sixth element either fires a potent action potential or shows a clearly subthreshold potential deflection. The SN element capacitance is set to 7/40 times the atrial element capacitance. This value is chosen somewhat arbitrarily so that the frequency at which the atrium is driven can vary wildly depending on the intercellular couplings, making tendencies clearly visible.

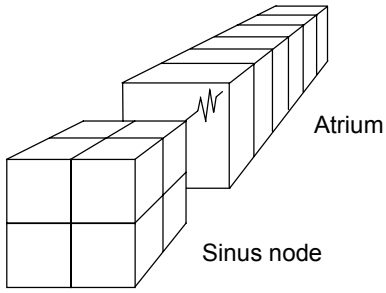

Fig. 2. The multi-element model used. A cube of eight SN elements is coupled to a row of six atrial elements via the uppermost right SN element.

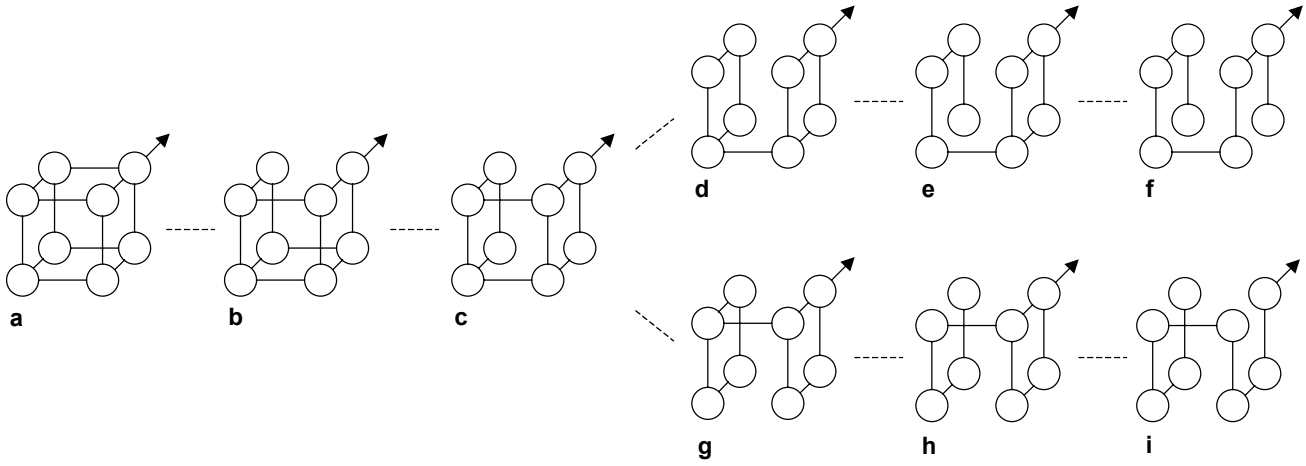

Fig. 3. Different coupling graphs for the eight SN elements in the cube in Fig. 2. Lines between circles represent gap junction connections between neighbour elements. The arrow in each panel indicates the impulse exit site to the atrium. Going from left to right, one connection is removed in each step, mimicking the presence of an increasing amount of isolating connective tissue strands.

The gap junction current j_{kl} from an element *k* to a neighbour element *l* is described as $j_{kl} = g_{kl}(V_k - V_l)$, with a constant conductance g_{kl}. Here V_k is the membrane potential of element *k*. Thus V_k follows

$$dV_k / dt = -(I_k + \sum_l j_{kl}) / C_k , \quad (1)$$

where I_k is the current flowing from element *k* to the extracellular fluidum and C_k is the membrane capacitance.

2.3. The numerical integration

In our model, the SA junction consists of a small SN element coupled to a large atrial element (Fig. 2). The large drain current to the atrium combined with the small capacitance of the SN element result in a large potential drop of the SN element per unit time due to the interaction across the junction. This may lead to divergence in a numerical integration. To overcome this problem, we used the integration method of Victorri et al. (1985), designed specifically to integrate Hodgkin-Huxley type equations. In this method, voltage changes are controlled in each step. In our version, if the voltage change $|\Delta V|$ of *any* SN element exceeds 0.5 mV, the time step Δt is halved and calculations redone. If $|\Delta V| < 0.25$ mV for *all* SN elements, Δt is doubled in *the next* iteration. Initially, Δt is set to 1 ms, and is not allowed to exceed this value. In a typical simulation, the mean time step is ≈ 0.1 ms. Occasionally, Δt drops to $2^{-6} \approx 0.016$ ms.

3. Results

3.1. The coupling between SN cells

Fig. 4 shows the behaviour of the system in the *gSA* – *gSS* parameter plane when coupling graph **a** in Fig. 3 is used. *gAA* is fixed to 150 S/F (conductance per unit *atrial* element capacitance). In the grey region, the outermost atrial element is successfully excited each time the SN elements fire, while in the white region, the atrium is silent. On the three curves inside the grey area, the atrium is driven at 600, 1300 and 2000 ms respectively. The lower, almost horizontal border between grey and white defines $gSA_{\min}$, the minimum *gSA* for which the atrium can be triggered. The vertical border to the left defines $gSS_{\min}$, the minimum *gSS* for successful triggering. There are very narrow regions just below $gSA_{\min}$ or $gSS_{\min}$ in which every second firing is transmitted to the atrium. It is possible to drive the atrium even for very high *gSS*, corresponding to an isopotential SN. However, the firing frequency increases if *gSA*

or *gSS* decrease. Therefore, if the safety factor to gSA_{min} is to be kept, to drive the atrium closer to the natural SN frequency, the small SN cells should be more weakly coupled.

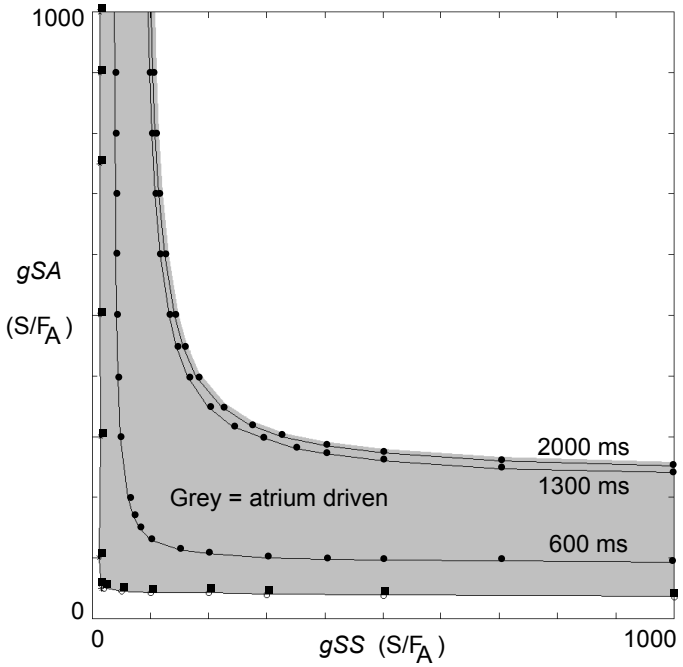

Fig. 4. Behaviour of the system in Fig. 2, with the SN elements coupled with common conductance *gSS* according to graph **a** in Fig. 3. *gSA* is the coupling between the uppermost right SN element and the atrial element closest to the SN. (Conductances are given per unit *atrial* element capacitance.) The eight SN elements are able to drive the atrium in the shaded parameter region. Along the three curves, the driving frequency is 600, 1300 and 2000 ms respectively. The firing frequency of the atrium increases if *gSA* or *gSS* decrease.

3.2. The connective tissue in the SN

However, if we reduce *gSS*, we drive the system closer to the critical gSS_{min}. In this subsection we test the hypothesis that the introduction of electrically insulating connective tissue strands allows a higher *gSS* without decreasing the driving frequency. In the coupling graphs **a** – **i** in Fig. 3, one connection is removed each step we take to the right. This corresponds to a successively increasing amount of connective tissue. Graph **a** can be imagined to correspond to lack of connective tissue, and is the one used to produce Fig. 4.

Fig. 5A shows the behaviour in the *gSS*-*gSA* plane when graph **e** is used (solid lines) compared to that of graph **a** (dashed lines). It is seen that the curve on which the driving frequency is 600 ms has shifted substantially to the right. gSS_{min} has also shifted to the right, but not as much. gSA_{min} is almost independent of the coupling graph.

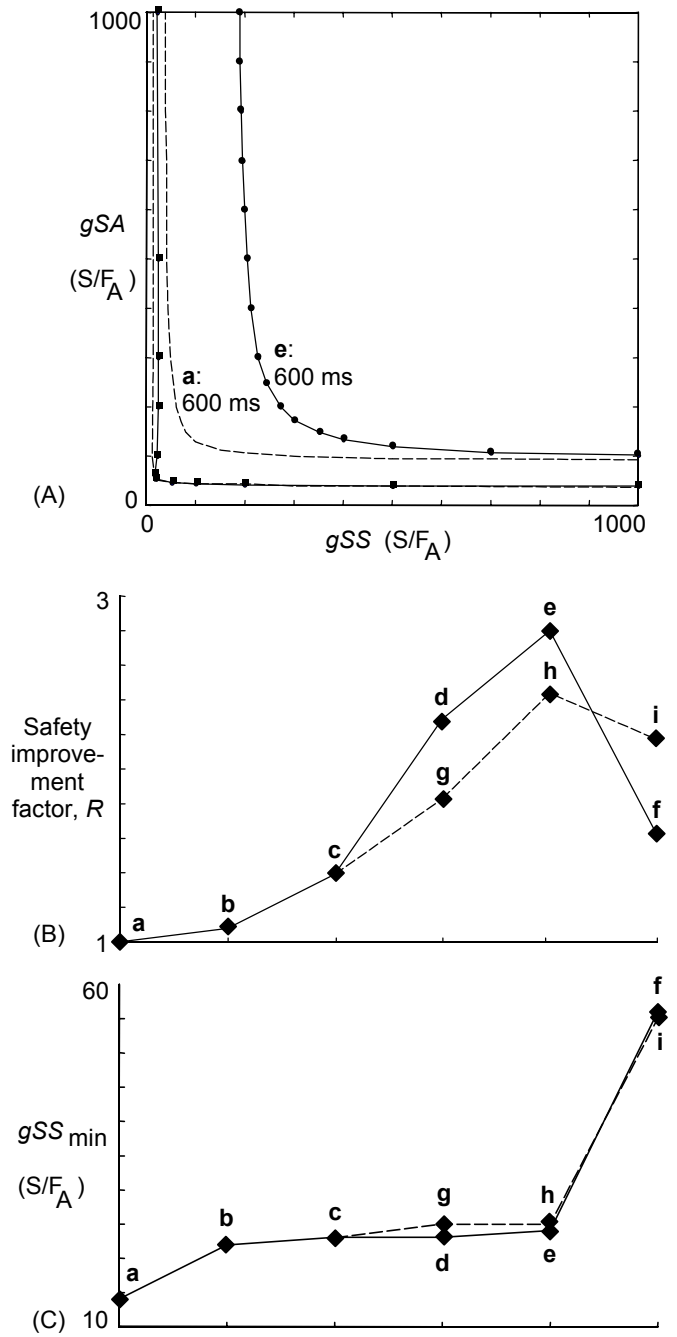

Fig. 5. Results of simulations in which the different coupling graphs in Fig. 3 are used. All couplings between SN elements have identical conductance *gSS*. (A) The behaviour of the system using graph **e** (solid lines), compared to that using graph **a** (dashed lines). The curve on which the driving frequency is 600 ms shifts substantially to the right due to the removal of some connections. gSS_{min}, the minimum *gSS* for which driving of the atrium is possible, also shifts to the right, but not as much. gSA_{min}, defined accordingly, remains practically unchanged. Thus, using coupling graph **e**, the atrium is driven at 600 ms intervals in a way such that the safety factors towards critically low *gSA* and *gSS* increase. (B) Safety improvement factor *R*, defined in Eqs. (2) and (3a), for the different coupling graphs. (C) gSS_{min} for each coupling graph in Fig. 3 at *gSA* = 500 S/F_A.

We define the safety factor $D(f, gSA)$ to $gSS_{\min}$ at a given driving frequency f and a given *gSA* as

$$D(f, gSA) = gSS_f / gSS_{\min}, \quad (2)$$

where gSS_f is the gSS which gives frequency f.

It is found that D is greater for graph **e** than for graph **a** for all f and all gSA. For example, $D_{\mathbf{e}}(600, 500) = 8.5$ whereas $D_{\mathbf{a}}(600, 500) = 3.04$. (The subscript refers to the graph.) The safety improvement factor R going from graph **x** to graph **y** is defined as

$$R = D_{\mathbf{y}}(600, 500) / D_{\mathbf{x}}(600, 500). \quad (3a)$$

Fig. 5B shows R going from graph **a** to the ones marked in the diagram. Electrically insulating connective tissue indeed seems to improve the functional safety of the SN. The trend is general – the diagram looks similar for every pre-chosen driving frequency f and SA coupling gSA. Note however that too much uncoupling may be unfavourable. For graphs **f** and **i**, where the SN elements are arranged in a one-dimensional chain, the safety factor D is less than in graphs **e** and **h**, for which the SN elements close to the SA junction are connected to a square. Fig. 5C illustrates that $gSS_{\min}$ mainly depends on the number of SN elements coupled to the junctional SN element. This number is three for graph **a**, two for graphs **b** – **e** and **g** – **h**, and one for graph **i**. It is also essentially one for graph **f**. These results are analysed further in the Discussion section.

A potential hazard when connective tissue strands are introduced is that they make it harder to achieve frequency entrainment among SN cells with varying natural frequency. To test the severity of this effect, the eight SN elements in the cube are assigned Q-values according to Fig. 6A. The range of resulting natural periods agrees reasonably with that among rabbit SN cells cells (Boyett et al., 1999; Boyett et al., 2000; Kodama and Boyett, 1985; Opthof et al., 1987). The atrium is disconnected, after which the minimum gSS giving frequency entrainment is measured for coupling graphs **a** – **f**. Fig. 6B shows that the critical gSS per unit *atrial* element capacitance increases from 0.27 to 0.65 S/F_A going from a three-dimensional coupling graph (**a**) to a one-dimensional (**f**).

However, $gSS_{\min} > 14$ S/F_A for all gSA and all graphs in Fig. 3. For those systems, $Q = 2$ for all SN elements. If some SN elements have a lower Q-value, as in the system in Fig. 6A, $gSS_{\min}$ has to be even higher. It may be concluded that whenever gSS is high enough to allow driving of the atrium, it is also high enough to entrain the SN element frequencies. This is

confirmed in simulations where the row of six atrial elements is connected to the system in Fig. 6A.

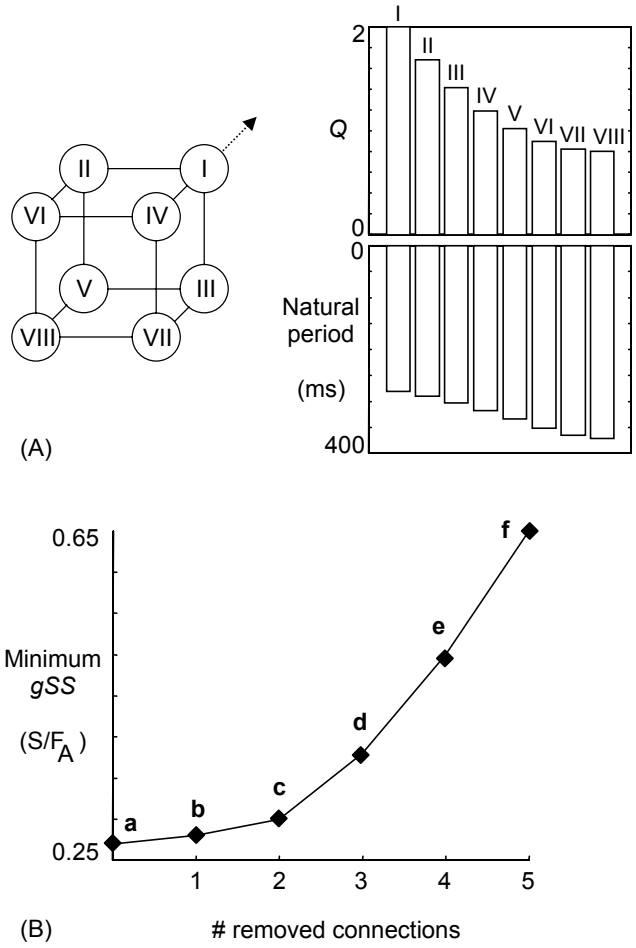

Fig. 6. Connective tissue increases the minimum *gSS* for which SN cells with varying natural frequencies become frequency entrained. (A) The eight SN elements are given different values of *Q*, which is the quotient between the actual membrane density of Ca- and K- channels and the normal density. Higher values of *Q* produce a higher natural frequency. The atrium is disconnected (indicated by a dotted arrow). (B) Minimum *gSS*, as defined above, for the different coupling graphs (Fig. 3). All couplings are equally strong.

3.3. The higher coupling between SN cells near the SA junction

The system in Fig. 2 with coupling graph **i** (a one-dimensional chain) is used. Fig. 7A shows the two ways in which couplings are altered. Along line 1), $g_5 - g_7$ are set a factor F higher than the couplings $g_1 = g_2 = g_3 = g_4 = gSS$. Along line 2), there is a linear gradient from $g_1 = gSS$ up to $g_7 = F \times gSS$.

As in Eq. (3a), a safety improvement factor R' is introduced as

$$R' = D_F(600, 500) / D_1(600, 500). \qquad (3b)$$

Here, the subscript of D refers to the coupling inhomogeneity factor F defined above. Fig. 7B displays R' as a function of F along lines 1) (solid) and 2) (dashed). It is seen that a big abrupt gap junction conductance increase close to the SA junction is the safest arrangement in the sense of large R'. When F increases, both gSS_{600} and gSS_{min} decrease, but gSS_{min} more rapidly, so that D increases [Eq. (2)]. The trends are general and do not depend upon the arguments of D or the coupling graph used.

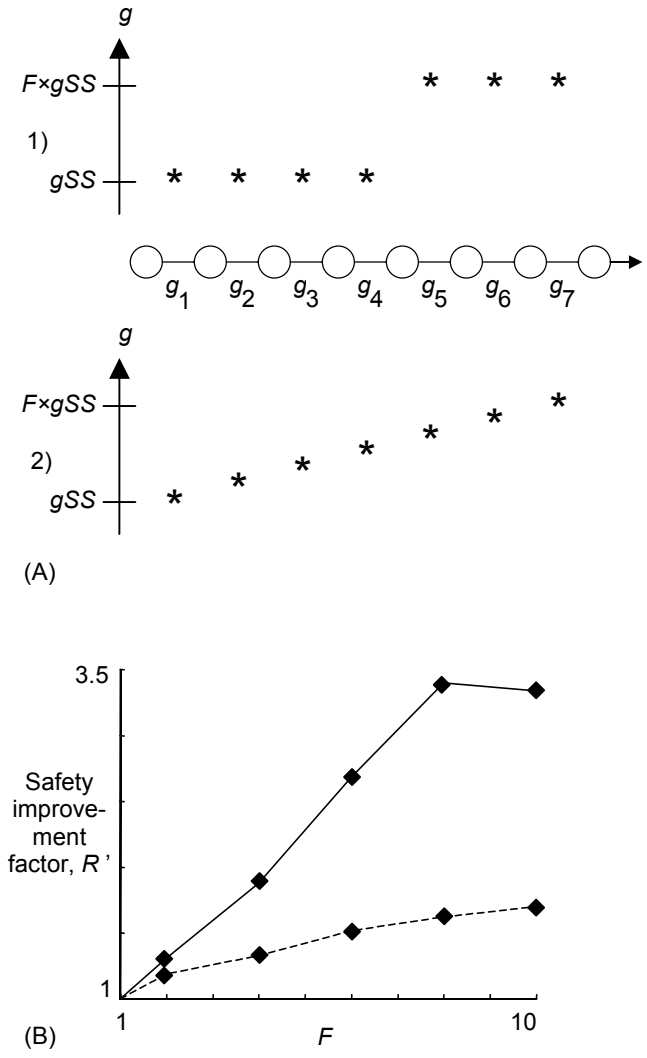

Fig. 7. Effects of higher coupling conductance close to the impulse exit sites than in the SN interior. (A) Coupling graph **i** (Fig. 3) is used. The arrow indicates the impulse exit site to the atrium. Along line 1), there is a discontinuous jump in coupling conductance from the SN interior to the periphery. Along line 2), there is a linear gradient. F defines the coupling inhomogeneity factor. (B) The safety improvement factor R' as a function of F along line 1) (solid line) and line 2) (dashed line). R' is defined in Eq. (3b).

4. Discussion

4.1. Role of weak coupling

It is not hard to see why reduced coupling between SN elements increases the frequency at which the atrium is driven. As long as coupling is high enough so that a firing of a SN element triggers the neighbours, the driving frequency is close to that of the innermost element, since that element is least affected by the drain. The drain experienced by this element decreases with decreasing coupling, so that the frequency increases.

4.2. Consequences of the connective tissue

The reason why the introduction of insulating connective tissue increases the driving frequency, if other parameters are kept constant, must be that it increases the electrical path length from an interior SN cell to the source of the drain – the SA junction. Some path lengths may not be increased, but the statement holds in the mean. The idea is illustrated in Fig. 8A. In our system, for coupling graph **a** (Fig. 3) there are three SN elements between the atrium and the innermost SN element, whereas for graph **i** there are seven. In the latter system, the innermost element experiences much lesser drain and attains a higher frequency. However, if the introduction of connective tissue is to be favourable in the sense that it increases the safety factor D [Eq. (2)] at a given ideal driving frequency f, gSS_f must increase with a greater factor than $gSS_{\min}$ does. In the simulations this is indeed the case. We now discuss why this may be so.

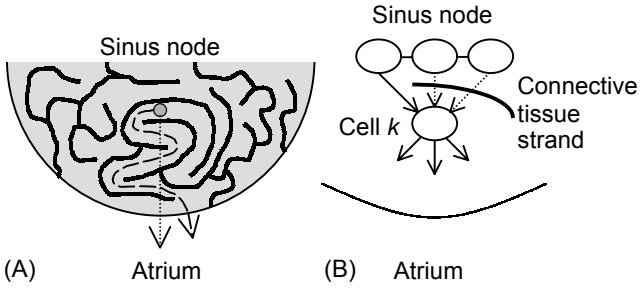

Fig. 8. (A) For many SN cells, isolating connective tissue strands increase the electric path length to the atrium. The cells sense less drain and fire at a higher frequency. (B) Illustration of the argument why gSS_{min} increases when connective tissue is introduced close to the SA junction. Cell k cannot fire if not triggered by the cells more interior to it. When two of these are disconnected, the remaining cell has to be more strongly coupled to accomplish the triggering.

The connective tissue may disconnect from a cell k some SN cells, which has *longer* path length to the atrium than cell k (Fig. 8B). Because of their longer path length, they fire before cell k. Suppose that cell k and the group of cells exposed to more drain than cell k are not able to fire at all if the more interior cells are decoupled. Then $gSS_{\min}$ is roughly the minimum gSS for which cell k is triggered collectively by the directly coupled more interior cells. When they fire, each such cell gives a pulse proportional to gSS. If n is the number of directly coupled more interior cells, then $gSS_{\min}$ should be roughly proportional to $1/n$. Fig. 5C indicates that $gSS_{\min}$ mainly depends on the number of SN elements directly coupled to the SA junctional SN element. For coupling graph **a** this number is three, for graphs **b** – **e** and **g** – **h** it is two, and for graphs **f** and **i** it is one. Strictly, it is two for graph **f**, but the element just beneath the junctional one has no connection to the SN interior, and turns out to be unable to fire by its own. Thus it does not help triggering the junctional element. Inspection of Fig. 5C then shows that the relation $gSS_{\min} \propto 1/n$ holds reasonably well if cell k is taken to be the junctional SN element. On the other hand, $gSS_{\min}$ remains almost constant if connections are removed further away from the junction (Fig. 5C). Since cells in this region experience less drain, they are more easily excited than the junctional cell, and they may also be able to fire by themselves. One might say that since the junctional SN element is hardest to trigger, $gSS_{\min}$ is determined by the number of couplings to this cell. That $gSS_{\min}$ remains constant when connective tissue is introduced further inside the SN, implies that D increases, since gSS_f increases, as discussed above. We think this can be stated quite generally, since it can be understood from general arguments.

Regarding connective tissue introduction very close to the SA junction, it is seen in Fig. 5B that D increases slightly going from graph **a** to graph **b**, whereas it *decreases* going from graph **e** to **f**, and from **h** to **i**. This is because during the operation, gSS_f does not increase as much as $gSS_{\min}$ does. Such operations are thus not necessarily favourable.

Analysing Fig. 5B further, the reason why graph **d** is more favourable than **g,** and **e** more favourable than **h**, is probably that for the former two, the path length for the innermost SN cell to the SA junction is longer. That graph **i** is better than graph **f** can be understood in the same way.

In judging which graph is to prefer, we have not considered the safety factor to $gSA_{\min}$. This is because $gSA_{\min}$ is essentially graph-independent (Fig. 5A). $gSA_{\min}$ is determined by the shape of the upshot of the junctional SN element. This is essentially an intrinsic cellular property, and depends little on external factors. gSA_f increases when more connective tissue is

introduced by the same reason as gSS_f does (increased path lengths to atrium). Therefore the safety factor to gSA_{min} always increases.

As discussed in section 3.2, a potential drawback with the connective tissue is that it makes it harder to achieve frequency entrainment at a given *gSS* (Fig. 6). However, when elements with different natural frequencies are used in our model system (Fig. 2B), these always entrain for a lower *gSS* than that for which the SN cells started to drive the atrium. This might be generally understood from the fact that the drain-induced frequency difference between the SA junctional SN cells and the interior ones is much greater than that between natural frequencies. Therefore a much larger coupling is needed to entrain the SN periphery to the interior, or, in our case, make it fire at all. In any case, desynchronisation among the SN cells due to the natural frequency differences just add a modest variation of firing intervals around a mean value close to that which would be seen if they did synchronize (Cai et al., 1994). Such a frequency variability would not put the health of the subject at hazard.

4.3. Why higher coupling near the SA junction may be advantageous

We argued that gSS_{min} mainly depends on the number of couplings to the SA junctional SN element, and is quite independent of the arrangement of the SN interior. In the same way, if the cell-to-cell coupling strengths are inhomogeneous, it seems that gSS_{min} depends mostly on the couplings between the SN cells closest to the SA junction. It turned out that for all inhomogeneity factors *F*, gSS_{min} occurred for $F \times gSS_{min} \approx 0.055$. Thus, we can reduce couplings in the SN interior without approaching gSS_{min}, thereby increasing the safety factor *D* [Eq. (2)], since the driving frequency increases due to the decreased drain experienced by the interior cells.

The reason why an abrupt coupling strength increase turned out to be better than a gradual one is not clear to us. The result is, however, in line with the finding of Cx43-positive SN cell bundles close to atrial cells (section 1).

4.4. Conclusions

Simulations and argumentation support the hypothesis that the following SN qualities have developed by evolutionary pressure to deal with the drain current to the atrium: 1) the weak intercellular coupling, 2) the great amount of connective tissue, and 3) the seemingly greater intercellular coupling close to impulse exit sites. The support for the hypothesis is in the form of found *tendencies* that the SN function *more* safely when these qualities are present. We have not attempted any quantitative statements of *how* safe the SN functions with and without

these qualities. The importance of the tendencies depends on the severity of the drain current, and in our view this question cannot yet be addressed by means of simulations.

As discussed in the Introduction, the strands of atrial tissue penetrating into the SN, and the more forceful peripheral SN cells can also be understood as measures to overcome the effects of the drain. That so many SN qualities can be accounted for in this way indicates that the drain indeed is often critical when the SN ceases to function properly. This hypothesis is consistent with the finding (Östborn et al., 2001a; Östborn et al. 2001b) that most arrhythmias associated with the sick sinus syndrome may appear as results of reduced intercellular coupling in the SN in the presence of severe drain.

Our simulations show that too much connective tissue close to the SA junction pushes the system closer to the limit where the atrium cannot be driven. Thus fibrosis of the SN can be one way in which the coupling is reduced below the level at which the SN cease to function properly. Indeed, Thery et al. (1977) found a correlation between fibrosis and the occurrence of sick sinus rhythms.

References

Bharati, S., Lev, M., 1988. Morphology of the sinus and atrioventricular nodes and their innervation. In: Mazgalev, T., Dreifus, L.S., Michelson, E.L. (Eds.), Electrophysiology of the Sinoatrial and Atrioventricular Nodes. Alan R. Liss, New York, pp. 3-14.

Bleeker, W.K., Mackaay, A.J., Masson-Pévet, M., Bouman, L.N., Becker, A.E., 1980. Functional and morphological organization of the rabbit sinus node. Circ. Res. 46, 11-22.

Bouman, L.N., Verheijck, E.E., van Ginneken, A.C.G., 1994. Atrio-sinus interaction in rabbit SA node demonstrated by blockade of delayed rectifier (I_K). J. Physiol. 479P, 68P.

Boyett, M., Holden, A.V., Kodama, I., Suzuki, R., Zhang, H., 1995. Atrial modulation of sinoatrial pacemaker rate. Chaos, Solitons & Fractals 5, 425-438.

Boyett, M.R., Honjo, H., Yamamoto, M., Nikmaram, M.R., Niwa, R., Kodama, I., 1999. Downward gradient in action potential duration along conduction path in and around the sinoatrial node. Am. J. Physiol. 276, H686-H698.

Boyett, M.R., Honjo, H., Kodama, I., 2000. The sinoatrial node, a heterogeneous pacemaker structure. Cardiovasc Res 47, 658-687.

Cai, D., Winslow, R.L., Noble, D., 1994. Effects of gap junction conductance on dynamics of sinoatrial node cells: two-cell and large-scale network models. IEEE Trans. Biomed. Eng. 41, 217-231.

Coppen, S.R., Kodama, I., Boyett, M.R., Dobrzynski, H., Takagishi, Y., Honjo, H., Yeh, H.I., Severs, N.J., 1999. Connexin45, a major connexin of the rabbit sinoatrial node, is co-expressed with connexin43 in a restricted zone at the nodal-crista terminalis border. J. Histochem. Cytochem. 47, 907-918.

De Mazière, A.M.G.L., van Ginneken, A.C.G., Wilders, R., Jongsma, H.J., Bouman, L.N., 1992. Spatial and functional relationship between myocytes and fibroblasts in the rabbit sinoatrial node. J. Mol. Cell. Cardiol. 24, 567-578.

Guevara, M.R., van Ginneken, A.C.G., Jongsma, H.J., 1987. Patterns of activity in a reduced ionic model of a cell from the rabbit sinoatrial node. In: Degn, H., Holden, A.V., Olsen, L.F. (Eds.), Chaos in Biological Systems. Plenum, London, pp. 5-12.

Irisawa, H., Noma, A., 1982. Pacemaker mechanisms of rabbit sinoatrial node cells. In: Bouman, L.N., Jongsma, H.J. (Eds.), Cardiac Rate and Rhythm. Nijhoff, The Hague, pp. 35-51.

James, T.N., 1977. The sinus node. Am. J. Cardiol. 40, 965-986.

Joyner, R.W., van Capelle, F.J.L., 1986. Propagation through electrically coupled cells: how a small SA node drives a large atrium. Biophys. J. 50, 1157-1164.

Joyner, R.W., Kumar, R., Golod, D.A., Wilders, R., Jongsma, H.J., Verheijck, E.E., Bouman, L., Goolsby, W.N., van Ginneken, A.C.G., 1998. Electrical interactions between a rabbit atrial cell and a nodal cell model. Am. J. Physiol. 274, H2152-H2162.

Kirchhof, C.J.H.J., Bonke, F.I.M., Allessie, M.A., Lammers, W.J.E.P., 1987. The influence of the atrial myocardium on impulse formation in the rabbit sinus node. Pflug. Arch. 410, 198-203.

Kodama, I., Boyett, M.R., 1985. Regional differences in the electrical activity of the rabbit sinus node. Pflug. Arch. 404, 214-226.

Kwong, K.F., Schuessler, R.B., Green, K.G., Laing, J.G., Beyer, E.C., Boineau, J.P., Saffitz, J.E., 1998. Differential expression of gap junction proteins in the canine sinus node. Circ. Res. 82, 604-612.

Masson-Pévet, M., Bleeker, W.K., Gros, D., 1979. The plasma membrane of leading pacemaker cells in the rabbit sinus node: A qualitative and quantitative ultrastructural analysis. Circ. Res. 45, 621-629.

Oosthoek, P.W., Virágh, S., Mayen, A.E.M., van Kempen, M.J.A., Lamers, W.H., Moorman, A.F.M., 1993. Immunohistological delineation of the conduction system I: the sinoatrial node. Circ. Res. 73, 473-481.

Opthof, T., van Ginneken, A.C.G., Bouman, L.N., Jongsma, H.J., 1987. The intrinsic cycle length in small pieces isolated from the rabbit sinoatrial node. J. Mol. Cell. Cardiol. 19, 923-934.

Östborn, P., Wohlfart, B., Ohlén, G., 2001. Arrhythmia as a result of poor intercellular coupling in the sinus node: a simulation study. J. Theor. Biol. 211, 201-217.

Östborn, P., Ohlén, G., Wohlfart, B., 2001. Simulated sinoatrial exit blocks explained by circle map analysis. J. Theor. Biol. 211, 219-227.

ten Velde, I., de Jonge, B., Verheijck, E.E., van Kempen, M.J.A., Analbers, L., Gros, D., Jongsma, H.J., 1995. Spatial distribution of connexin43, the major cardiac gap junction protein, visualizes the cellular network for impulse propagation from sinoatrial node to atrium. Circ. Res. 76, 802-811.

Thery, C., Gosselin, B., Lekieffre, J., Warembourg, H., 1977. Pathology of sinoatrial node. Correlations with electrocardiographic findings in 111 patients. Am. Heart. J. 93, 735-740.

Verheijck, E.E., Wessels, A., van Ginneken, A.C.G., Bourier, J., Markman, M.W.M., Vermeulen, J.L.M., de Bakker J.M.T., Lamers, W.H., Opthof, T., Bouman, L.N., 1998. Distribution of atrial and nodal cells within the rabbit sinoatrial node. Models of sinoatrial transition. Circulation 97, 1623-1631.

Verheijck, E.E., van Kempen, M.J.A., Veereschild, M., Lurvink, J., Jongsma, H.J., Bouman, L.N., 2001. Electrophysiological features of the mouse sinoatrial node in relation to connexin distribution. Cardiovasc. Res. 52, 40-50.

Verheule, S., van Kempen, M.J.A., Postma, S., Rook, M.B., Jongsma, H.J., 2001. Gap junctions in the rabbit sinoatrial node. Am. J. Physiol. 280, H2103-H2115.

Victorri, B., Vinet, A., Roberge, F.A., Drouhard, J.P., 1985. Numerical integration of cardiac action potentials using Hodgkin-Huxley-type models. Comp. Biomed. Res. 18, 10-23.

Watanabe, E.I., Honjo, H., Anno, T., Boyett, M.R., Kodama, I., Toyama, J., 1995. Modulation of pacemaker activity of sinoatrial node cells by electrical load imposed by an atrial cell model. Am. J. Physiol. 269, H1735-H1742.

Wohlfart, B., Arlock, P., 1993. Simulation of the electrogram from ion currents. Clin. Physiol. 13, 441-451.

Zhang, H., Holden, A.V., Kodama, I., Honjo, H., Lei, M., Varghese, T., Boyett, M.R., 2000. Mathematical models of action potentials in the periphery and center of the rabbit sinoatrial node. Am. J. Physiol. 279, H397-H421.

Zhang, H., Boyett, M.R., Holden, A.V., Honjo, H., Kodama, I., 1998. Evidence that the Na^+ current, i_{Na}, in the periphery of the sinoatrial node helps the node drive the surrounding atrial muscle. J. Physiol. 506P, 54P-55P.